ISSN 1983-1838
(DOI): 10.18624/etech.v16i1.1276

EFFECT OF METAL INERT GAS ARC WELDING ON MECHANICAL PROPERTIES OF A UNS S41003 STAINLESS STEEL

EFEITO DE SOLDAGEM A ARCO ELÉTRICO COM PROTEÇÃO GASOSA INERTE NAS PROPRIEDADES MECÂNICAS DE UM AÇO INOXIDÁVEL UNS S41003

JOSÉ CARLOS DE LACERDA
https://orcid.org/0000-0001-7753-1713 / http://lattes.cnpq.br/6449312240961537 / jlacerda@unifei.edu.br
Universidade Federal de Itajubá - UNIFEI, Itabira, Minas Gerais

RICARDO LUIZ PEREZ TEIXEIRA
https://orcid.org/0000-0003-2641-4036/ http:// http://lattes.cnpq.br/0937037728177696/ ricardo.luiz@unifei.edu.br
Universidade Federal de Itajubá- UNIFEI, Itabira, Minas Gerais

ANDRÉ GOMES ROCHA
https://orcid.org/0000-0003-4699-9895 / http://lattes.cnpq.br/9254616053538746 / andregomeerocha@gmail.com
Universidade Federal de Itajubá - UNIFEI, Itabira, Minas Gerais

DIEGO FELLIPE RODRIGUES DA SILVA
https://orcid.org/0000-0001-5898-9702 / http://lattes.cnpq.br/5709153760118467 / engenheirodiegofellipe@gmail.com
Universidade Federal de Itajubá- UNIFEI, Itabira, Minas Gerais

VINICIUS SAYEG REIS SOUSA
https://orcid.org/0000-0001-5677-4038 / http://lattes.cnpq.br/8675081566848712/ reissayeg@gmail.com
Universidade Federal de Itajubá - UNIFEI, Itabira, Minas Gerais

Recebido em: 12/08/2023.
Aprovado em: 16/09/2023.
Publicado em: 11/10/2023.

ABSTRACT

In this work, the effects of metal inert gas (MIG) welding on the microstructure and mechanical properties of a UNS S41003 steel were studied. UNS S41003 steel sheets were welded with AISI 309LSi wire using two different welding energies: high energy (HE) and low energy (LE). Samples extracted from the base metal (BM), heat affected zone (HAZ), and fused zone (FZ) were subjected to microhardness and Charpy impact tests. Tensile tests were performed on samples extracted from the BM. Micrographic analyses of the structures obtained in the welds were performed using scanning electron microscopy (SEM). Microfractographic images of tensile and impact fractures were obtained by scanning electron microscopy (SEM). As a result, the predominance of austenitic microstructure with the presence of delta ferrite islands was observed in the FZ. In HAZ there was a pronounced increase in the grain size of the ferrite phase with the existence of laths

ISSN 1983-1838
(DOI): 10.18624/etech.v16i1.1276

eTECH
TECNOLOGIAS PARA
COMPETITIVIDADE INDUSTRIAL

EFFECT OF METAL INERT GAS ARC WELDING ON MECHANICAL PROPERTIES OF A UNS S41003 STAINLESS STEEL

JOSÉ CARLOS DE LACERDA
RICARDO LUIZ PEREZ TEIXEIRA
ANDRÉ GOMES ROCHA
DIEGO FELLIPE RODRIGUES DA SILVA
VINICIUS SAYEG REIS SOUSA

martensite predominantly in its grain boundary. The BM showed greater hardness than the metal from the FZ and HAZ. The impact toughness was higher in the FZ compared to BM and HAZ.
Keywords: UNS S41003; MIG welding; mechanical properties; microstructure.

1 INTRODUCTION

The stainless steel UNS S41003 has been presented as an excellent substitute for carbon steels in several applications in the sugar and alcohol industry and more recently also in the manufacture of concrete mixers (DE FARIA et al., 2020). The use of this stainless steel, compared to carbon steels, favors the weight reduction of the installations by the application of smaller resistant sections. This is possible due to its higher mechanical strength and greater resistance to abrasion and corrosion, compared to carbon steels. This reduction in the weight of the structures with the use of UNS S41003 steel instead of carbon steel has a direct impact on the reduction of operating costs with fuels used in the transport and operation of the equipment. It is also necessary to consider the reduction of maintenance costs due to the longer useful life of the equipment motivated by its greater resistance to corrosion and abrasion comparted with carbon steels (DE FARIA et al., 2020; MARIÓ, 2008).

Mainly due to its low carbon content, UNS S41003 steel has a good weldability characteristic (ZHANG et al., 2015). This steel is normally ferritic; however, depending on the heat treatment conditions, it may have a mixed ferrite/martensite structure. From the volumetric fraction of the ferrite/martensite phases, it is possible to optimize the performance of steel in its different applications. The possibility of obtaining the ferrite/martensite phases in UNS S41003 steel is due to the low concentrations of chromium and other ferrite stabilizing elements in its chemical composition. In this case, the existence of an austenite stability field in an intercritical temperature range is favored. As the steel UNS S41003 is susceptible to austenitic transformation in a certain temperature range, with appropriate heat treatment, different fractions of the ferrite/austenite phases can be obtained. Then, depending on the cooling rate, there may be a consequent transformation of austenite into martensite (DE FARIA et al., 2020; CASHELL, BADDOO, 2014).

As shown, the ferrite/martensite microstructure in UNS S41003 steel can be obtained by performing quench treatment at intercritical temperatures from the original ferritic microstructure of the steel. In this case, the steel is heated to a certain temperature in the range of A_{c1} (initial austenitization temperature) to A_{c3} (final austenitization temperature) and soon after this is followed by rapid cooling. The greater the temperature and the austenitization time applied in the heat treatment within the mentioned temperature range, the greater the volumetric fraction of martensitic phase (DE FARIA et al., 2020).

Considering the above in relation to the possibility of UNS S41003 steel to produce a two-phase microstructure by heat treatment, this can have an impact on effects produced by welding on the steel. In the various applications of UNS S41003 steel, it is very common to use electric arc welding with gas shielding (ZHENG et al., 2010). In this case, depending on the welding parameters used (voltage, current, and electric arc displacement speed), microstructural changes may occur in the weld region.

ISSN 1983-1838
(DOI): 10.18624/etech.v16i1.1276

JOSÉ CARLOS DE LACERDA
RICARDO LUIZ PEREZ TEIXEIRA
ANDRÉ GOMES ROCHA
DIEGO FELLIPE RODRIGUES DA SILVA
VINICIUS SAYEG REIS SOUSA

Grain growth, embrittlement, and sensitization are the main problems in the HAZ of welds of ferritic stainless steels with low carbon and chromium contents, such as the UNS S41003 steel. These microstructures transformations result in reduced impact toughness properties at low temperatures and intergranular corrosion resistance (ZHENG et al., 2010). Therefore, in this work, the effects on the microstructure and mechanical properties of UNS S41003 steel welded by the MIG process will be studied.

The present work was motivated for a better understanding of the behavior of UNS S41003 steel when it is welded. As reported, this steel is ferritic, so the grain growth in its HAZ is very favorable (CASHELL & BADDOO, 2014). In addition, this steel presents susceptibility to martensitic transformation in a certain intercritical temperature range (DE FARIA et al., 2020). The combination of these two situations when UNS S41003 steel is welded needs to be better known and there are few publications in this regard.

It is believed that the scientific and technological information generated by this work will contribute to better guidance in the applications of UNS S41003 steel, especially those where welding is involved. The information generated by science and transformed into technology is essential for competitiveness due to the innovation it can leverage (ZSCHORNACK et al., 2019).

2 EXPERIMENTAL PROCEDURES

The stainless steel UNS S41003 has been presented as an excellent substitute for carbon steels in several applications in the sugar and alcohol industry and more recently also in the manufacture of concrete mixers (DE FARIA et al., 2020). The use of this stainless steel, compared to carbon steels, favors the weight reduction of the installations by the application of smaller resistant sections. This is possible due to its higher mechanical strength and greater resistance to abrasion and corrosion, compared to carbon steels. This reduction in the weight of the structures with the use of UNS S41003 steel instead of carbon steel has a direct impact on the reduction of operating costs with fuels used in the transport and operation of the equipment. It is also necessary to consider the reduction of maintenance costs due to the longer useful life of the equipment motivated by its greater resistance to corrosion and abrasion (DE FARIA et al., 2020; MARIÓ, 2008).

Mainly due to its low carbon content, UNS S41003 steel has a good weldability characteristic (ZHENG et al., 2010). This steel is normally ferritic; however, depending on the heat treatment conditions, it may have a mixed ferrite/martensite structure. From the volumetric fraction of the ferrite/martensite phases, it is possible to optimize the performance of steel in its different applications. The possibility of obtaining the ferrite/martensite phases in UNS S41003 steel is due to the low concentrations of chromium and other ferrite stabilizing elements in its chemical composition (DE FARIA et al., 2020; CASHELL & BADDOO, 2014). In this case, the existence of an austenite stability field in an intercritical temperature range is favored. As a result, as steel is susceptible to austenitic transformation in a certain temperature range, with appropriate heat treatment, different fractions of the ferrite/austenite phases can be obtained. Then, depending on the cooling rate, there may be a consequent transformation of austenite into martensite (DE FARIA et al., 2020; CASHELL & BADDOO, 2014).

ISSN 1983-1838
(DOI): 10.18624/etech.v16i1.1276

JOSÉ CARLOS DE LACERDA
RICARDO LUIZ PEREZ TEIXEIRA
ANDRÉ GOMES ROCHA
DIEGO FELLIPE RODRIGUES DA SILVA
VINICIUS SAYEG REIS SOUSA

As shown, the ferrite/martensite microstructure in UNS S41003 steel can be obtained by performing quench treatment at intercritical temperatures from the original ferritic microstructure of the steel. In this case, the steel is heated to a certain temperature in the range of A_{c1} (initial austenitization temperature) to A_{c3} (final austenitization temperature) and soon after this is followed by rapid cooling. The greater the temperature and the austenitization time applied in the heat treatment within the mentioned temperature range, the greater the volumetric fraction of martensitic phase (DE FARIA et al., 2020.

Considering the above in relation to the possibility of UNS S41003 steel to produce a two-phase microstructure by heat treatment, this can have an impact on effects produced by welding on the steel. In the various applications of UNS S41003 steel, it is very common to use electric arc welding with gas shielding (ZHENG et al.2010). In this case, depending on the welding parameters used (voltage, current, and electric arc displacement speed), microstructural changes may occur in the weld region.

Grain growth, embrittlement, and sensitization are the main problems in the HAZ of welds of ferritic stainless steels with low carbon and chromium contents, such as the UNS S41003 steel. These microstructures transformations result in reduced impact toughness properties at low temperatures and intergranular corrosion resistance (ZHENG et al., 2010). Therefore, in this work, the effects on the microstructure and mechanical properties of UNS S41003 steel welded by the MIG process will be studied.

As base metal for the welds, stainless steel sheets UNS S41003 in the dimensions of 200 mm x 150 mm x 4.75 mm were used. As filler metal, AISI 309LSi austenitic stainless steel solid wire, 0.9 mm in diameter, was used. Tables 1 and 2 show the chemical compositions of UNS S41003 steel and AISI 309LSi welding wire. The chemicals compositions of the UNS S41003 and AISI 309LSi weld wire were obtained by optical emission spectroscopy (OES). Welding was performed using the metal inert-gas (MIG) process. The welding parameters are shown in Table 3. The shielding gas used was argon with 2% oxygen, with a flow rate of 17 l/min.

Table 1 - Chemical composition of UNS S41003 steel (% by mass)

C	Mn	Si	P	Cr	Ni	Mo	Cu	Co	N
0.01%	0.55%	0.53%	0.03%	11.01%	0.31%	0.02%	0.06%	0.02%	130 ppm

Source: The authors (2023)

Table 2 - Chemical composition of AISI 309LSi welding wire (% by mass)

C	Cr	Ni	Mn	Mo	Si	P	Cu
0.03	24.1	13.3	1.55	0.75	0.75	0.03	0.66

Source: The authors (2023)

ISSN 1983-1838
(DOI): 10.18624/etech.v16i1.1276

EFFECT OF METAL INERT GAS ARC WELDING ON MECHANICAL PROPERTIES OF A UNS S41003 STAINLESS STEEL

JOSÉ CARLOS DE LACERDA
RICARDO LUIZ PEREZ TEIXEIRA
ANDRÉ GOMES ROCHA
DIEGO FELLIPE RODRIGUES DA SILVA
VINICIUS SAYEG REIS SOUSA

Table 3 - Welding parameters

WELDING ENERGY	VOLTAGE (V)	CURRENT (A)	WIRE FEED SPEED (mm/s)	WELDING SPEED (mm/min)	GAS FLOW (L/min)	STICK OUT (mm)
HIGH (47.8 J/cm)	24.4	196	200	100	17	25
LOW (23.9 J/cm)	24.4	196	200	200	17	25

Source: The authors (2023)

The welds were performed using a machine model Smaseld-316, brand ESAB. For carrying out welds, a table equipped with an automatic system to control the displacement of the welding torch was used (Figure 1). During the welding, special care was taken to ensure that the welding speed, voltage, current, gas flow, wire feed speed, and stick-out remained constant.

Figure 1 - Experimental welding table

Source: The authors (2023)

The experimental procedures consisted of the following steps: preparation of joints for welding; welding execution; machining of specimens; tensile tests; microhardness tests; Charpy impact tests; micrographic analysis of weld regions; analysis of tensile fracture; and analysis of Charpy impact fracture.

Before welding, the sheets were subjected to a careful cleaning with acetone to eliminate contamination of the joints with oil or any other impurities from the sheet rolling and chamfer machining processes. The use of a butt joint welded in flat position was adopted to obtain weld regions that favored the location of the notches of the specimens for the Charpy impact tests on the

ISSN 1983-1838
(DOI): 10.18624/etech.v16i1.1276

EFFECT OF METAL INERT GAS ARC WELDING ON MECHANICAL PROPERTIES OF A UNS S41003 STAINLESS STEEL

JOSÉ CARLOS DE LACERDA
RICARDO LUIZ PEREZ TEIXEIRA
ANDRÉ GOMES ROCHA
DIEGO FELLIPE RODRIGUES DA SILVA
VINICIUS SAYEG REIS SOUSA

HAZ and FZ. Two welding procedures were used in order to obtain samples welded with two energies (high energy and low energy), as shown in Table 3.

The specimens for the tensile tests, Charpy impact tests, and micrographic analyses were prepared using a machining process by electrical discharge using a molybdenum wire in the EUROSTEC machine, model EURO FW2. Tensile tests were performed on the base metal using strain control at a speed of 2 mm/min. Three specimens were tested and a universal testing system machine (EMIC brand, model DL10000) was used. The specimens used in the tensile tests were sub-size according to ASTM E8/E8M (1995)[6]. The specimens were machined at the plate thickness as received (4.75 mm), as shown in Figure 2. The Charpy impact test specimens were machined according to ASTM E23-96, in the thickness of the plate as received (4.75 mm), as shown in Figure 3.

Figure 2 - Tensile test specimen (dimensions in mm)

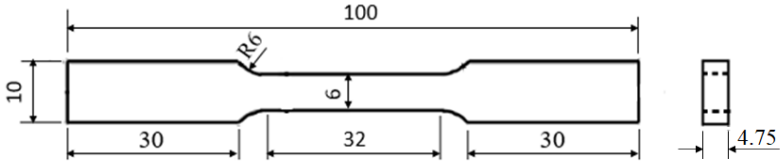

Source: The authors (2023)

Figure 3 - Charpy impact specimen (dimensions in mm)

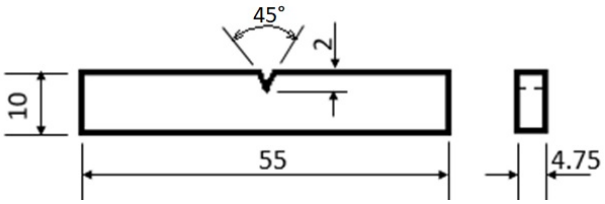

Source: The authors (2023)

For the microstructural characterizations, specimens were extracted from the welds, embedded in Bakelite and subsequently subjected to metallographic preparation by sanding with 120# to 1200# sandpaper. After this step, there was polishing with 0.25 µm diamond paste. Aqua regia chemical attack etching was used. For the metallographic images, scanning electron microscopy (SEM) was used.

For a better understanding of the UNS S41003 steel, simulation of microstructural transformations was performed using the *ThermoCalc™* software, considering the chemical composition of the steel shown in Table 1.

ISSN 1983-1838
(DOI): 10.18624/etech.v16i1.1276

EFFECT OF METAL INERT GAS ARC WELDING ON MECHANICAL PROPERTIES OF A UNS S41003 STAINLESS STEEL

JOSÉ CARLOS DE LACERDA
RICARDO LUIZ PEREZ TEIXEIRA
ANDRÉ GOMES ROCHA
DIEGO FELLIPE RODRIGUES DA SILVA
VINICIUS SAYEG REIS SOUSA

3 RESULTS AND DISCUSSION

As reported, the UNS S41003 steel is ferritic, but it can to present martensitic transformation with heat treatment in the intercritical temperature range of austenitization followed by rapid cooling. Figure 4 presents a phase equilibrium diagram of UNS S41003 steel obtained by numerical simulation carried out by *ThermoCalc*™ software.

Figure 4 - Phase equilibrium diagram of UNS S41003 steel obtained by simulation carried out by ThermoCalc™

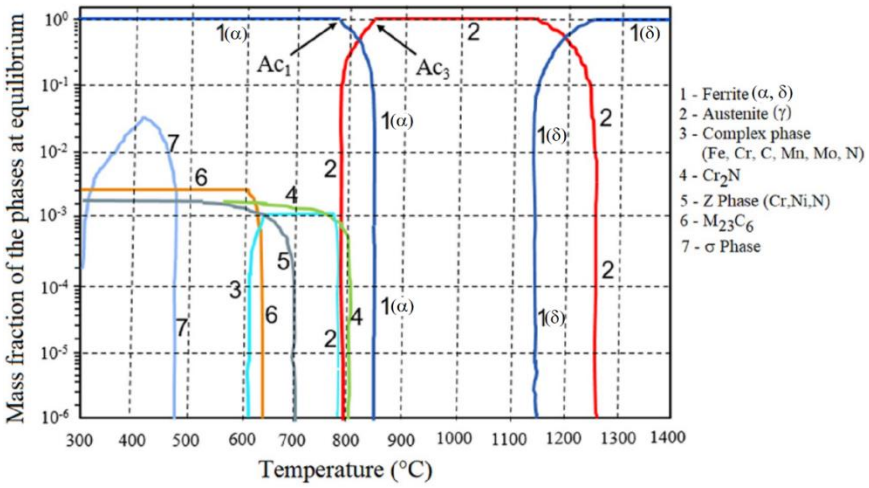

Source: The authors (2023)

According to the phase diagram shown in Figure 4, above approximately 1240°C there is a microstructure with 100% delta ferrite (δ). Between approximately 1240°C and 1170°C there is the presence of delta ferrite and austenite in fractions that vary according to the temperature in this intercritical range. In the temperature range between 1170°C and 860°C the microstructure is 100% austenitic. Below approximately 860°C (A_{c3}), the increasing precipitation of the ferritic phase begins within the austenitic matrix. In this case, in the range of 860°C (A_{c3}) and 780°C (A_{c1}), the volumetric fraction of ferrite increases as the temperature decreases until it reaches close to 100% at the end point of ferritic transformation (A_{c1}).

Below 780°C (A_{c1}), the microstructure is very close to 100% ferritic phase with the possibility of very low fractions of other deleterious phases such as: complex phases (Fe-Cr-C-Mn-Mo-N), Z phase (Cr-Ni-N), Cr_2N, $M_{23}C_6$, and sigma phase (σ). The susceptibility to the formation of the mentioned deleterious phases is more favored in the cooling in the equilibrium. Thus, in the case of welding, as there are high continuous cooling rates, the formation of these phases is more difficult. However, the high cooling rates produced by welding could facilitate the formation of martensite due

ISSN 1983-1838
(DOI): 10.18624/etech.v16i1.1276

EFFECT OF METAL INERT GAS ARC WELDING ON MECHANICAL PROPERTIES OF A UNS S41003 STAINLESS STEEL

JOSÉ CARLOS DE LACERDA
RICARDO LUIZ PEREZ TEIXEIRA
ANDRÉ GOMES ROCHA
DIEGO FELLIPE RODRIGUES DA SILVA
VINICIUS SAYEG REIS SOUSA

to the eventual austenitic transformation in the intercritical temperature range located between 860°C and 780°C, as reported.

The microstructural transformations analyzed in the phase diagram of Figure 4 occur at equilibrium, that is, under conditions of slow cooling. However, in the case of welding, there are typically high continuous cooling rates. In this case, the prediction of microstructures in welded joints of stainless steels can be performed using the Schaeffler diagram (ZHANG, Di et al., 2020), as shown in Figure 5. Figure 5 shows the prediction of microstructures in the regions of welded joints of the UNS S41003 steel, using the Schaeffler diagram. In the plotted Cr_{eq} and Ni_{eq} points of the low energy weld fused zone (FZ-LE), high energy weld fused zone (FZ-HE) and heat affected zone (HAZ), the respective predicted microstructures are identified. In this case, the existence of austenite + ferrite is observed in the FZ-LE and FZ-HE and ferrite + martensite in the HAZ.

Figure 5 - Schaeffler diagram: prediction of microstructure in welded joints of UNS S41003 steel

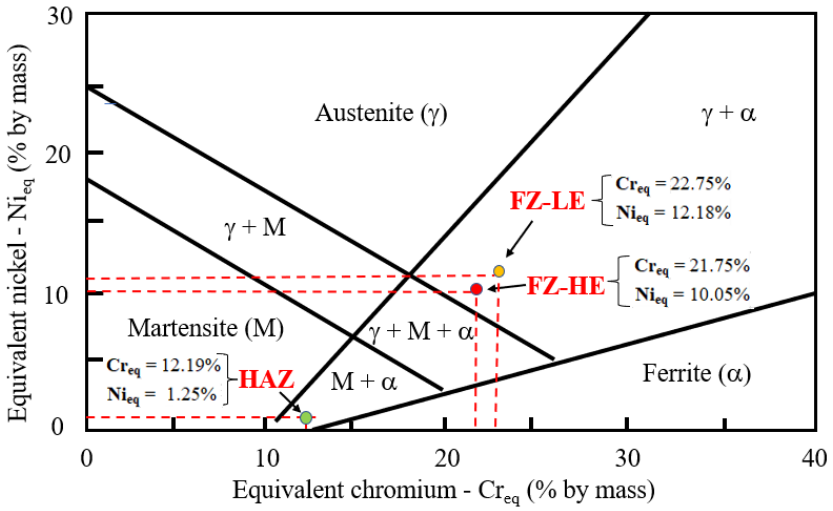

Source: The authors (2023)

Equivalente chromium (Cr_{eq}) and equivalente nickel (Ni_{eq}) in the FZ-LE, FZ-HE and HAZ were calculated using Equations 1 and 2, respectively (ZHANG, Di et al., 2020).

$$Cr_{eq} = Cr + 2Si + 1.5Mo + 5V + 5.5Al + 1.75Nb + 1.5Ti + 0.75W \quad (1)$$

$$Ni_{eq} = Ni + Co + 30C + 25N + 0.5Mn + 0.3Cu \quad (2)$$

The chemical compositions of the alloys formed in the FZ-LE and FZ-HE were calculated from the respective dilutions in the welds (FZ-LE = 27%; FZ-HE = 37%) considering the chemical compositions of the base metal and the weld wire used, presented in Tables 1 and 2.

3.1 Weld microstructure

In the two welding conditions (low and high energy) there was a pronounced increase in the ferrite grain size in the weld heat affected zone (HAZ) compared to the base metal (BM) (Figure 6-

ISSN 1983-1838
(DOI): 10.18624/etech.v16i1.1276

JOSÉ CARLOS DE LACERDA
RICARDO LUIZ PEREZ TEIXEIRA
ANDRÉ GOMES ROCHA
DIEGO FELLIPE RODRIGUES DA SILVA
VINICIUS SAYEG REIS SOUSA

a, b). The average ferrite grain diameter in the HAZ, calculated according to ASTM E-112, was approximately 330 μm and 410 μm in the low and high energy welds, respectively. The average ferrite grains diameter calculated in the base metal (BM) was 4.7 μm. The presence of laths martensite in the grain boundaries of the ferrite grain in the welds HAZ region can also be observed, as highlighted by arrows in Figure 6(a, b). The ferrite phase is very susceptible to grain growth in the HAZ (LAKSHMINARAYANA & BALASUBRAMANIAN. 2012; LIPPOLD & KOTEC. 2005; DE FÁTIMA ARRUDA. 2021).

Figure 6 - Welding joints microstructures: (a) low energy; (b) high energy (SEM)

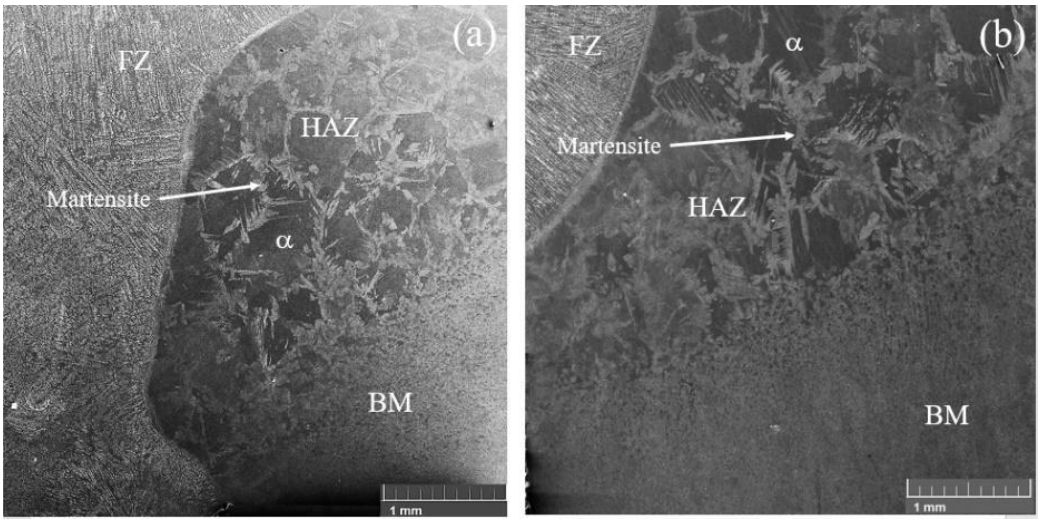

Source: The authors (2023)

Figure 7 shows the microstructure of the base metal (BM) formed by a ferritic phase with refined grain (≈ 4.7 μm).

ISSN 1983-1838
(DOI): 10.18624/etech.v16i1.1276

EFFECT OF METAL INERT GAS ARC WELDING ON MECHANICAL PROPERTIES OF A UNS S41003 STAINLESS STEEL

JOSÉ CARLOS DE LACERDA
RICARDO LUIZ PEREZ TEIXEIRA
ANDRÉ GOMES ROCHA
DIEGO FELLIPE RODRIGUES DA SILVA
VINICIUS SAYEG REIS SOUSA

Figure 7 - Base metal microstructure (SEM)

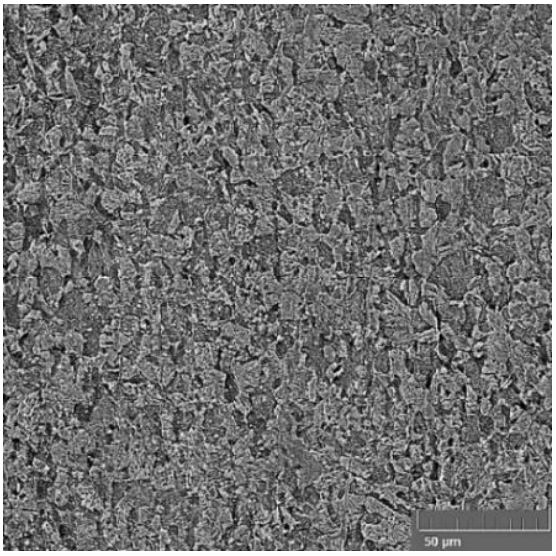

Source: The authors (2023)

The fused zones of both welds (low and high energy) showed structures constituted by the presence of islands of delta ferrite phase dispersed in the austenitic phase matrix, as shown in Figure 8. The presence of these two phases was due to the dilution that occurred in the welds where, in this case, the austenite phase came from the welding wire (AISI 309LSi) and the ferrite phase came from the base metal (UNS S41003). The two welding energy conditions produced two different values of dilution in the FZ: ≈ 37% in the high-energy weld and ≈ 27% in the low-energy weld. The dilution values were calculated from the ratio of the volume of BM that melted in the FZ. The volumetric fraction of ferrite phase was 38±1% and 28 ±2% in the FZ of high energy and low energy welds, respectively, according to ASTM 562E [13]. In Figure 8(a, b) the difference in the distribution morphology of the ferritic phase in the matrix of the austenitic phase is highlighted in yellow. A greater field of refinement of the microstructure of the FZ of the high energy welding can be observed (Figure 8-b) compared to the FZ of the low energy welding (Figure 8-a).

ISSN 1983-1838
(DOI): 10.18624/etech.v16i1.1276

JOSÉ CARLOS DE LACERDA
RICARDO LUIZ PEREZ TEIXEIRA
ANDRÉ GOMES ROCHA
DIEGO FELLIPE RODRIGUES DA SILVA
VINICIUS SAYEG REIS SOUSA

Figure 8 - Fused zone microstructure: (a) low energy welding; (b) high energy welding (SEM)

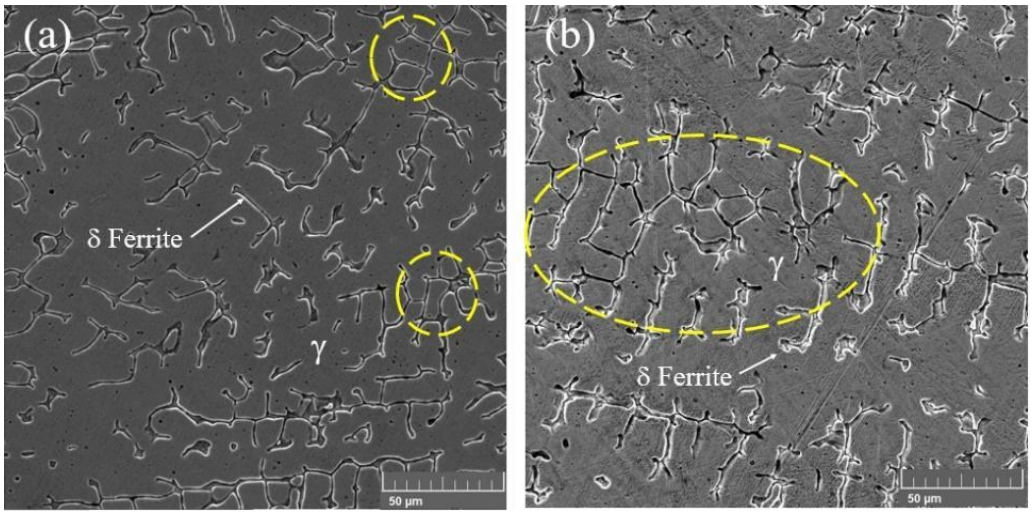

Source: The authors (2023)

3.2 Tensile mechanical properties

Figure 9 shows the engineering stress-strain curve obtained by tensile testing performed on UNS S41003 steel used as base metal in MIG welding. Table 4 presents the main results of mechanical properties of the steel obtained from the tensile test.

Figure 9 - UNS S41003 steel base metal tensile stress–strain curve

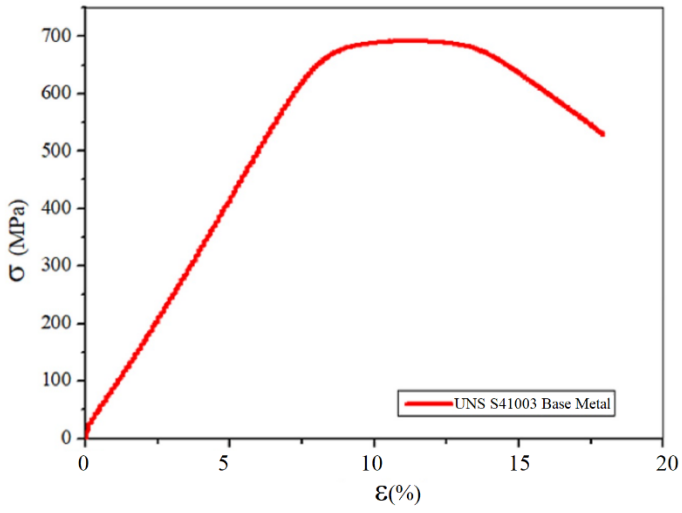

ISSN 1983-1838
(DOI): 10.18624/etech.v16i1.1276

EFFECT OF METAL INERT GAS ARC WELDING ON MECHANICAL PROPERTIES OF A UNS S41003 STAINLESS STEEL

JOSÉ CARLOS DE LACERDA
RICARDO LUIZ PEREZ TEIXEIRA
ANDRÉ GOMES ROCHA
DIEGO FELLIPE RODRIGUES DA SILVA
VINICIUS SAYEG REIS SOUSA

Source: The authors (2023)

Table 4 - UNS S41003 steel base metal tensile mechanical properties

σ_{YS} (MPa)	σ_{UTS} (MPa)	ε(%)
648 ± 14	692 ± 12	18.4 ± 0.3

(σ_{YS}: yield stress; σ_{UTS}: ultimate tensile stress; ε: total strain)

Source: The authors (2023)

In Figure 10(a, b), fracture images of UNS S41003 steel (base metal) tested by tension are shown. In Figure 10(a) a pronounced deformation by necking can be observed, indicating the predominance of ductile fracture. The existence of a secondary crack in the direction of lamination of the plate can also be observed. This type of secondary crack can be caused by delamination due to the existence of aligned inclusions, chemical segregation, or preferential precipitation of phases towards lamination resulting from the thermomechanical processing of steel (DE FÁTIMA ARRUDA, 2021).

Figure 10 - UNS S41003 steel microfractography tested by tension: (a) necking region; (b) region with dimples and cleavage (SEM)

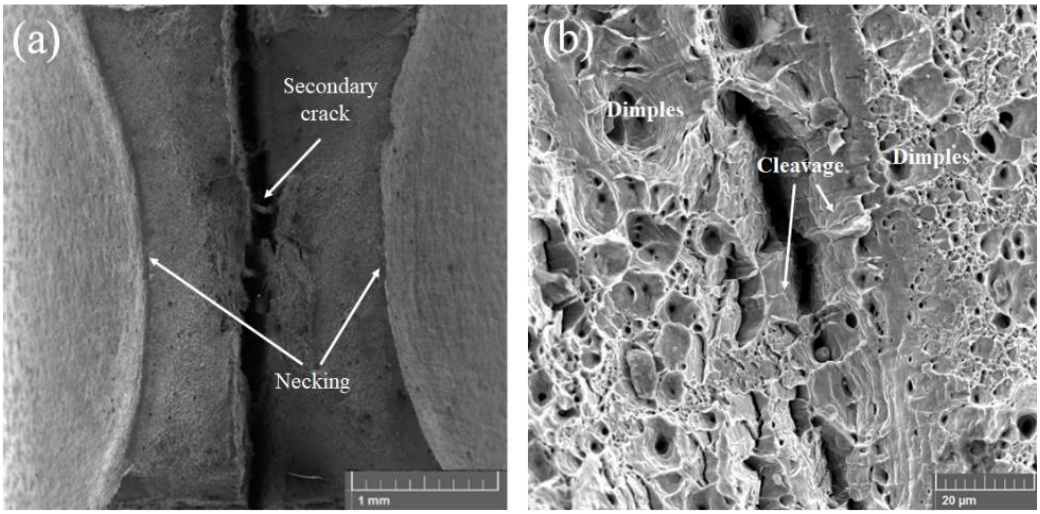

Source: The authors (2023)

In Figure 10(b), it can be observed that the fracture presents a predominance of ductile characteristics with small regions presenting brittle fracture behavior. There are dimples probably nucleated from carbides precipitated inside the grains. These dimples are caused by the growth of

ISSN 1983-1838
(DOI): 10.18624/etech.v16i1.1276

JOSÉ CARLOS DE LACERDA
RICARDO LUIZ PEREZ TEIXEIRA
ANDRÉ GOMES ROCHA
DIEGO FELLIPE RODRIGUES DA SILVA
VINICIUS SAYEG REIS SOUSA

microvoids that coalesce. The existence of dimples indicates a ductile fracture characteristic. In regions close to the secondary crack, there is a fracture with a compatible morphology of brittle behavior identified by the presence of cleavage facets. In these regions, there is an aspect of a distinct cracking mechanism that indicates sliding of crystallographic planes (ANDERSON, 2017; LIU et al, 2022).

3.3 Weld microhardness

Figure 11 shows the Vickers microhardness profile of the welds. The base metal (BM) showed greater hardness than the metal in the fused zone (FZ) and in the heat affected zone (HAZ) due to its smaller grain size (average grain diameter ≈ 4.7 μm). The HAZ metal from the low energy weld showed higher microhardness values compared to the HAZ metal from the high energy weld. This result can be attributed to the smaller ferrite grain size in HAZ-LE (330 μm) compared to HAZ-HE (410 μm).

Figure 11 - Microhardness profile of high and low energy welds

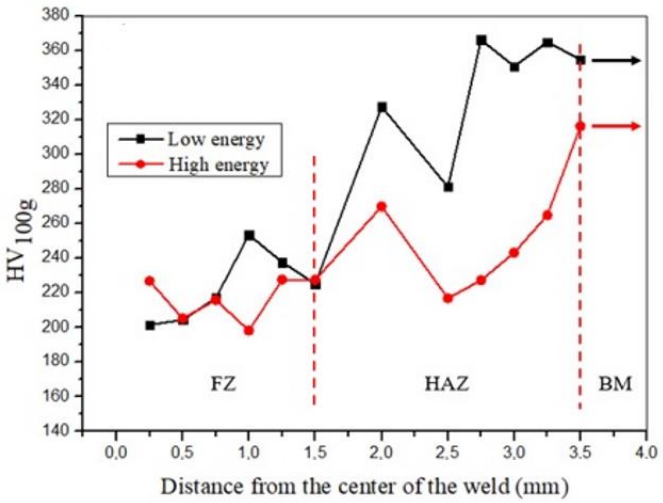

Source: The authors (2023)

3.4 Impact resistance

Figure 12 shows the results of energy absorbed in the Charpy impact tests with the notches located in the welded joints (BM, HAZ, and FZ) in the two welding energy conditions used (LE and HE). Charpy impact tests were performed at room temperature. The higher energy absorbed in Charpy impact tests in the FZ, compared to the BM, can be attributed to the presence of the austenite phase in the FZ.

Greater Charpy impact energy absorption can be observed in the FZ of the HE weld compared to the Charpy impact energy absorbed in the LE weld. This higher Charpy impact energy absorption observed in the FZ of the HE weld can be attributed to the existence of larger

ISSN 1983-1838
(DOI): 10.18624/etech.v16i1.1276

microstructure fields with finer grains in the FZ of the HE weld compared to the FZ of the LE weld, as shown highlighted by circles and ellipse in Figure 8. The high impact energy absorbed in the Charpy tests on the HAZ of the HE weld was probably influenced by the high impact strength of the FZ. Finally, the lower impact resistance observed in the BM was due to its structure being formed only by the ferritic phase LIU et al, 2022).

Figure 12 - Charpy test impact energy on welded joints

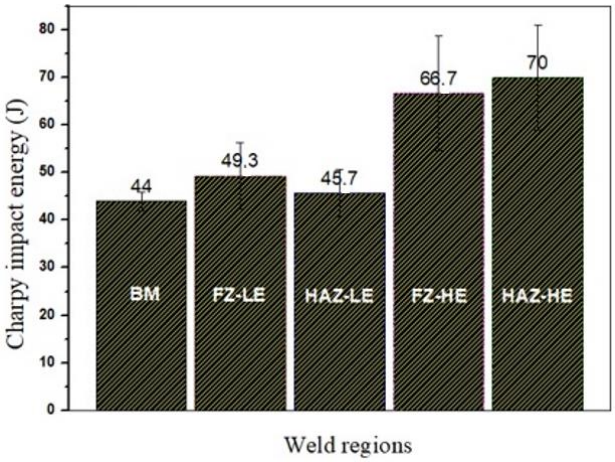

Source: The authors (2023)

Figure 13 shows images of the Charpy impact test base metal fracture. As highlighted in Figure 13, there was the formation of a secondary crack in the central region of the fracture, similarly occurred in the fracture by tensile test. As already reported, secondary cracks of this type can be caused by delamination due to the existence of aligned inclusions, chemical segregation, or preferential precipitation of phases towards lamination resulting from the thermomechanical processing of steel (DE FÁTIMA ARRUDA, 2021). According to the morphology of the fracture, it presented a mixed characteristic of ductile and brittle fracture behavior. There are regions with the presence of dimples (indicative of ductile behavior) and others with the existence of cleavage facets (indicating brittle behavior) (Figure 13 b, c). In Figure 13 (b) it is possible to observe dimples in the region of grain boundaries delimiting cleavages produced within the grain.

ISSN 1983-1838
(DOI): 10.18624/etech.v16i1.1276

Figure 13 - Charpy impact test fracture in the base metal (SEM)

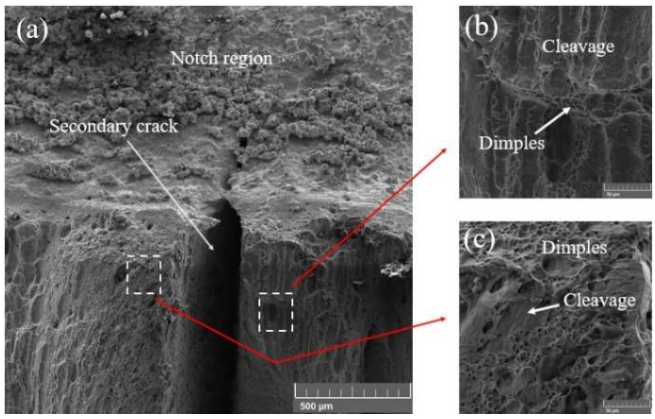

Source: The authors (2023)

Figure 14 shows the Charpy impact test fracture in the low energy weld heat affected zone (HAZ-LE). As can be seen in Figure 14(b), the main fracture mechanism was due to cleavage, but there were small regions where small dimples occurred, as highlighted. Transgranular cleavage facets occurred, as is typical of a ferritic phase, and even more with large grain size as was the case in the HAZ of the high energy weld (average grain diameter = 410 µm)[16]. Dimples occurred mainly in the adjacencies of grain boundaries where there was probably a higher concentration of inclusions, chemical segregation, or precipitation. These concentrations of inclusions, segregations, or precipitates favored the nucleation and coalescence of microvoids that favored the formation of dimples [14]. Another observation to be considered is in relation to the occurrence of a secondary crack (highlighted in Figure 14-a) similar which occurred in the tensile fracture of the base metal (highlighted in Figure 10a). As already reported, this type of secondary crack may have been caused by delamination due to the existence of aligned inclusions, chemical segregation, or preferential precipitation of phases towards lamination resulting from the thermomechanical processing of steel (DE FÁTIMA ARRUDA, 2021).

ISSN 1983-1838
(DOI): 10.18624/etech.v16i1.1276

EFFECT OF METAL INERT GAS ARC WELDING ON MECHANICAL PROPERTIES OF A UNS S41003 STAINLESS STEEL

JOSÉ CARLOS DE LACERDA
RICARDO LUIZ PEREZ TEIXEIRA
ANDRÉ GOMES ROCHA
DIEGO FELLIPE RODRIGUES DA SILVA
VINICIUS SAYEG REIS SOUSA

Figure 14 - Charpy impact test fracture in the HAZ of the high energy weld (SEM)

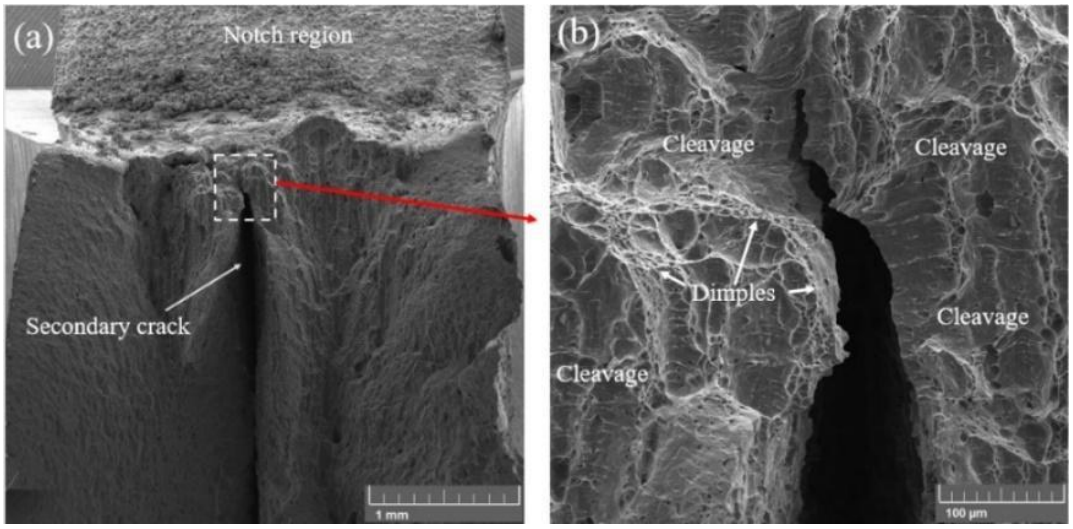

Source: The authors (2023)

In Figure 15, images of the fracture occurring in the fused zone of the high energy weld (FZ-HE) after the Charpy impact test are shown. Figure 15(b) shows the predominance of dimples resulting from the nucleation and coalescence of microvoids from inclusion particles or precipitates in the microstructure, as highlighted by arrows (ANDERSON, 2017. The fracture morphology presented in Figure 15 is consistent with what was expected for the FZ-HE, considering its microstructure with 38% ferrite and 62% austenite phases (LAUKKANEN et al., 2021).

Figure 15 - Charpy impact test fracture in the FZ of the high energy weld (SEM)

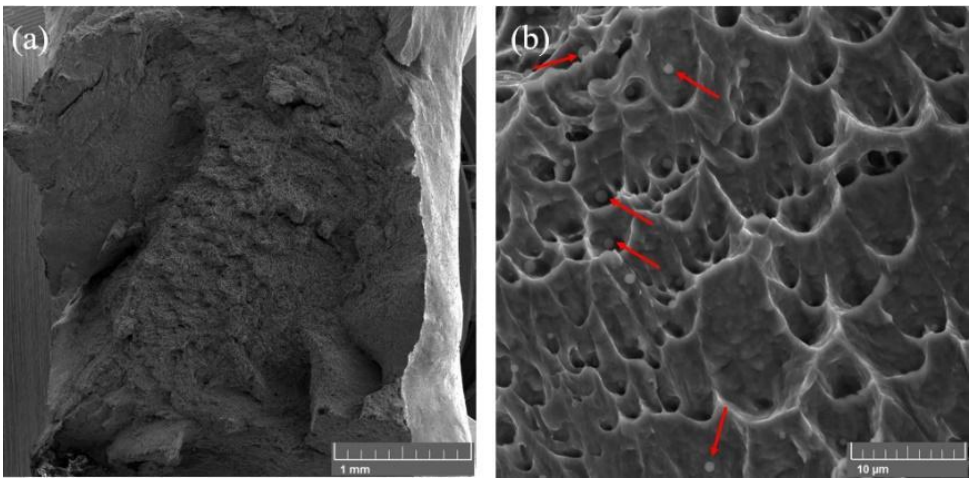

Source: The authors (2023)

ISSN 1983-1838
(DOI): 10.18624/etech.v16i1.1276

3 CONCLUSION

According to the results obtained in the present work, it was possible to observe that there was a pronounced ferrite grain growth was observed in the HAZ of the welds compared to the base metal. There was martensite in the grain boundaries of the ferrite in the HAZ, probably motivated by the partial transformation of austenite formed by heating. The FZ of both welds (low and high energy) showed phases constituted by the presence of delta ferrite phase islands dispersed in the austenitic phase matrix. In the fracture from the Charpy impact and tensile tests, the existence of secondary cracking in the direction of lamination of the sheet was observed, probably caused by delamination. The BM showed higher hardness than the FZ and HAZ of both welds due to its smaller grain size. The HAZ metal from the low energy weld showed higher microhardness values compared to the HAZ metal from the high energy weld due to its smaller grain size. The austenitic phase present in the FZ of the welds contributed to their greater resistance to Charpy impact tests compared to BM.

For future work, it is suggested to carry out selective electrochemical tests in the respective regions of the welds to identify corrosion potentials, pitting potentials and degrees of sensitization.

REFERENCES

ANDERSON, Ted L. **Fracture mechanics: fundamentals and applications**. CRC press, 2017.

ASTM E112-96. Standard test methods for determining average grain size. (1996).

ASTM E23-96. Standard test methods for notched bar impact testing of metallic materials. (1996).

ASTM E8M-95. Standard test method for tension testing of metallic materials (metric). (1995).

CASHELL, K. A.; Baddoo, N. R. Ferritic stainless steels in structural applications. **Thin-Walled Structures**, v. 83, p. 169-181, 2014.

DE FARIA, Geraldo Lucio et al. Effect of martensite volume fraction on the mechanical behavior of an UNS S41003 dual-phase stainless steel. **Materials Science and Engineering: A**, v. 797, p. 140208, 2020.

DE FÁTIMA ARRUDA, Amanda Aparecida et al. Influência da temperatura sobre o comportamento mecânico do aço inoxidável ferrítico ASTM A240 UNS S41003. **Tecnologia em Metalurgia, Materiais e Mineração**, v. 18, p. 0-0, 2021.

LAKSHMINARAYANAN, A. K.; Balasubramanian, V. Assessment of fatigue life and crack growth resistance of friction stir welded AISI 409M ferritic stainless steel joints. **Materials Science and Engineering: A**, v. 539, p. 143-153, 2012.

LAUKKANEN, Anssi et al. Micromechanics driven design of ferritic–austenitic duplex stainless steel microstructures for improved cleavage fracture toughness. **Engineering Fracture Mechanics**, v. 253, p. 107878, 2021.

ISSN 1983-1838
(DOI): 10.18624/etech.v16i1.1276

LIPPOLD, John C.; Kotecki, Damian J. **Welding metallurgy and weldability of stainless steels**. 2005.

LIU, B. P. et al. Effect of thermal aging on the microstructure and mechanical property of 410S ferritic stainless steel. **Materials Science and Engineering: A**, v. 856, p. 143952, 2022.

MARIÓ, H.C. Aços Inoxidáveis: aplicações e especificações. **São Paulo: Arcelor Mittal Inox Brasil**, 2008.

ZHANG, Di et al. Additive manufacturing of duplex stainless steels-a critical review. **Journal of Manufacturing Processes**, v. 73, p. 496-517, 2022.

ZHANG, Zhaohan et al. Microstructure evolution in heat affected zone of T4003 ferritic stainless steel. **Materials & Design**, v. 68, p. 114-120, 2015.

ZHENG, Huaibei et al. Study on microstructure of low carbon 12% chromium stainless steel in high temperature heat-affected zone. **Materials & Design**, v. 31, n. 10, p. 4836-4841, 2010.

ZSCHORNACK, Thiago et al. Observatório de inovação como ferramenta de subsídio à inteligência nas organizações. **Revista e-TECH: Tecnologias para Competitividade Industrial-ISSN-1983-1838**, v. 12, n. 1, p. 7-22, 2019.